Int. J. Multiphase Flow Vol. 12, No. 1, pp. 115–126, 1986
Printed in Great Britain.

0301–9322/86 $3.00 + .00

STRUCTURE OF TURBULENT BUBBLY JETS—II. PHASE PROPERTY PROFILES

T-Y. SUN and G. M. FAETH

Department of Mechanical Engineering and The Applied Research Laboratory, The Pennsylvania State University, University Park, PA 16802, U.S.A.

(*Received* 5 *September* 1984; *in revised form* 28 *April* 1985)

Abstract—This is the second part of a two-part study reporting structure measurements in bubbly turbulent round jets in a still environment. Measurements are compared with three theoretical approaches: (1) locally homogeneous flow analysis, where velocity differences between the phases were neglected; (2) deterministic separated flow analysis, where relative velocity was considered but bubble/turbulence interactions were ignored; and (3) stochastic separated flow analysis, where both relative velocity and bubble/turbulence interactions were considered using random-walk methods. This part of the study considers measurements and predictions of mean and fluctuating phase velocities and mean bubble number intensities at several axial stations. Locally homogeneous flow analysis was not very satisfactory since effects of relative velocity were important for present test conditions. Deterministic separated flow analysis was also ineffective, since neglecting turbulent dispersion caused the width of the bubble-containing region to be underestimated. In contrast, the stochastic separated flow analysis yielded reasonably good predictions.

1. INTRODUCTION

The objective of this investigation was to obtain a better understanding of turbulent bubbly free-shear flow. Measurements were made of the structure of dilute, turbulent, bubbly round jets, injected vertically upward in a still environment. Several analyses of the process were also considered, both to assist interpretation of the measurements and to initiate baseline evaluation of models using the new data.

This is the second part of a two-part paper describing the study. The first part considered theoretical and experimental methods; calibration results for the motion of single bubbles and single-phase jets; initial conditions for the flows; and mean phase velocities along the axis of the bubbly jets (Sun & Faeth 1985). The present paper reports mean and fluctuating phase velocities and mean bubble number intensities; sensitivity analysis of predictions; and effects of bubbles on continuous-phase turbulence properties (called turbulence modulation by Al Taweel & Landau 1977).

Three bubbly air/water jets were considered, primarily distinguished by their gas-volume fraction at the injector exit, e.g., case I, 2.4%; case II, 4.8%; and case III, 9.1%. All jets were turbulent, having initial Reynolds numbers in the range 8740–9380. The injector exit diameter was 5.08 mm. Bubbles within the jets had nearly uniform diameters of roughly 1 mm. Measurements were made of mean and fluctuating phase velocities using laser Doppler anemometry (LDA) and distribution of bubbles using flash photography. Complete specification of the flows and experimental methods are presented by Sun (1985) and Sun & Faeth (1985).

Three methods of analysis were considered: (1) locally homogeneous flow (LHF) analysis, where velocity differences (slip) between the phases were neglected; (2) deterministic separated flow (DSF) analysis where relative velocity was considered but bubble/turbulence interactions were ignored; and (3) stochastic separated flow (SSF) analysis, where both relative velocity and bubble/turbulence interactions were considered using random-walk methods. The general approach used in these analyses was developed during earlier studies of particle-laden jets by Shuen et al. (1983, 1983a, 1985). Present consideration of bubbly jets introduces effects of virtual mass and Basset forces which are small for particle-laden jets or sprays in gases.

Theoretical and experimental methods, as well as notation, are described in the companion paper by Sun & Faeth (1985) and will not be repeated here. The present paper considers the new structure measurements; effects of turbulence modulation; and the sensitivity of predictions to uncertainties in initial conditions and dispersed-phase parameters. A complete tabulation of data is provided by Sun (1985).

2. STRUCTURE MEASUREMENTS AND PREDICTIONS

2.1 *General description*

In the following, structure measurements and predictions are presented as mass(Favre)-averages, defined as follows:

$$\tilde{\phi} = \overline{\rho\phi}/\bar{\rho}. \quad [1]$$

This procedure is necessary in order to correctly represent predictions of the LHF analysis, which treats the bubbly jets as variable-density single-phase flows. Favre- and time-averages are identical for separate liquid- or gas-phase properties, and are essentially the same in any event since the maximum density variation in the present flows was only 10%.

LHF computations were initiated at the injector exit; however, the separated-flow calculations were initiated at $x/d = 8$, which was the position nearest the injector exit where needed measurements could be made. Effects of Basset forces and turbulence modulation were small for present test conditions (Sun & Faeth 1985); therefore, these phenomena were ignored in computed separated flow results illustrated here. However, results of computations considering turbulence modulation are described.

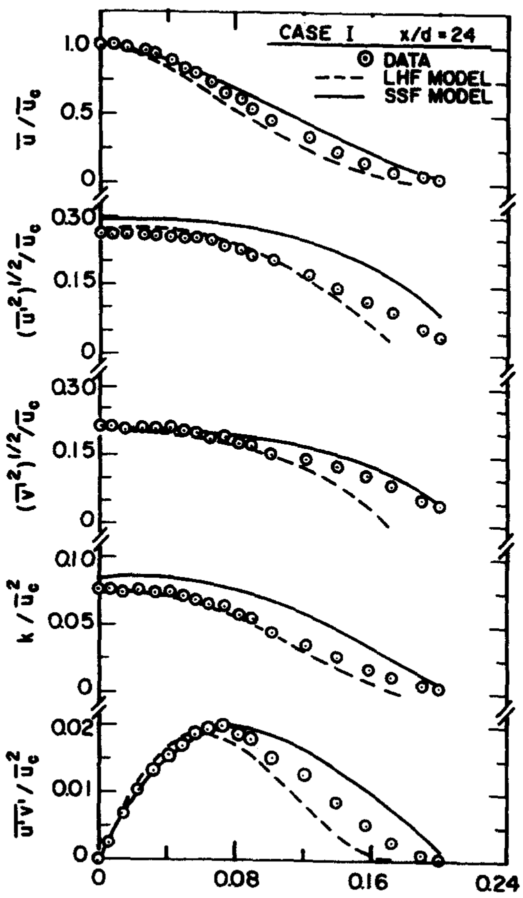

Figure 1. Mean and turbulent liquid-phase properties for the case I bubbly jet at $x/d = 24$.

2.2 *Structure*

Continuous-phase properties. In addition to measurements of initial conditions at $x/d = 8$ and along the flow axes, discussed by Sun & Faeth (1985), flow properties were also measured at $x/d = 24$, 40 and 60. Results at $x/d = 24$ and 40 will be emphasized here, since effects of tank confinement are smallest at these positions.

Measurements and predictions (LHF and SSF analyses) of mean and fluctuating continuous-phase properties for the case I and III bubbly jets are presented in figures 1–4. Mean streamwise velocity, streamwise and radial velocity fluctuations, turbulence kinetic energy (assuming equal radial and tangential velocity fluctuations) and Reynolds stress are illustrated. Measurements are plotted as a function of r/x, which is the similarity variable for fully developed turbulent jets. Predictions of continuous-phase properties for both separated-flow analyses are nearly identical for all the flows. The turbulence model used for the continuous phase does not yield separate predictions of velocity fluctuations; therefore, these estimates were obtained assuming $\tilde{u}'^2{:}\tilde{v}'^2 = k{:}k/2$, which are the usual ratios observed in fully developed single-phase jets, cf. Wygnanski & Fiedler (1969).

When plotted in the manner shown in figures 1–4, differences between the LHF and SSF analyses are not large. However, centerline velocities (which are used to normalize all the predictions) are overestimated by the LHF analysis while they are predicted reasonably well by the separated flow analyses; therefore, the separated flow analyses yield best quantitative agreement between predictions and measurements.

By comparing figures 1 and 2 with figures 3 and 4, it can be seen that levels of anisotropy of $\tilde{u}'$ and $\tilde{v}'$ are similar to single-phase jets for the case I bubbly jet but are appreciably

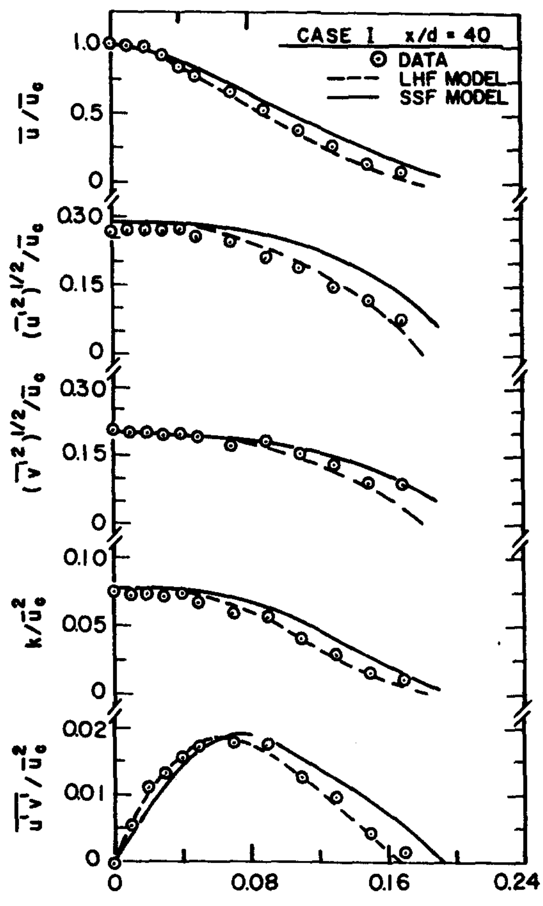

Figure 2. Mean and turbulent liquid-phase properties for the case I bubbly jet at $x/d = 40$.

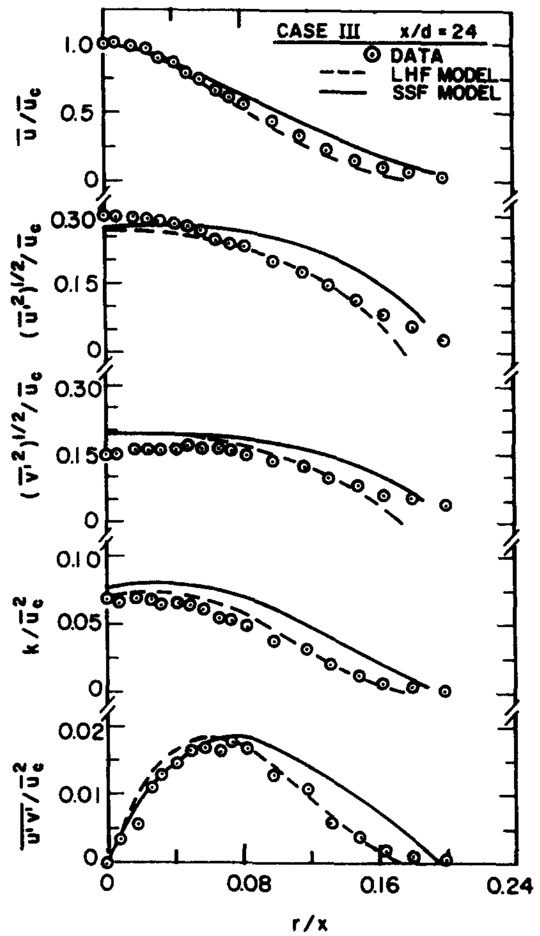

Figure 3. Mean and turbulent liquid-phase properties for the case III bubbly jet at $x/d = 24$.

increased for the case III jet. Furthermore, values of $\tilde{u}'/\tilde{u}_c$, $k/\tilde{u}_c^2$ and $\overline{u'v'}/\tilde{u}_c^2$ are increased 10–15% for the case III jet in comparison to the case I jet. These changes are probably due to effects of increased buoyancy in the higher-void fraction case III jet, e.g., similar behavior has been observed in buoyant plumes (Jeng & Faeth 1984). Increased levels of anisotropy have also been observed in regions of nonevaporating sprays having high drop densities, possibly due to preferential exchange of streamwise momentum (which is enhanced by buoyancy in the present case) from the dispersed phase, cf. Solomon *et al.* (1984). Treating these effects in a more complete manner requires use of a multistress turbulence model, or a full simulation of the turbulent flow, as well as consideration of effects of turbulence modulation. The latter effect will be discussed later.

Dispersed-phase properties. Predicted and measured dispersed-phase properties for the case I and III bubbly jets appear in figures 5–8. The results consist of mean and fluctuating streamwise bubble velocities. Mean velocity predictions are illustrated for all three analyses, with DSF predictions terminated at the predicted edge of the bubble-containing region (denoted by an arrow). The DSF model ignores bubble–turbulence interactions; therefore, this approach yields no estimate of bubble fluctuating velocities. Levels of continuous-phase and bubble velocity fluctuations are assumed to be the same in the LHF analysis; therefore $\tilde{U}_p'^2 = \tilde{u}'^2 = k$, consistent with earlier practice for the continuous phase.

The mean bubble velocity predictions of the separated flow-analyses are in good agreement with the measurements, cf. figures 5–8. A major defect of the DSF approach, however, is that it substantially underestimates the spread of bubble phase, since effects of turbulent dispersion of bubbles are ignored. The DSF approach actually corresponds to

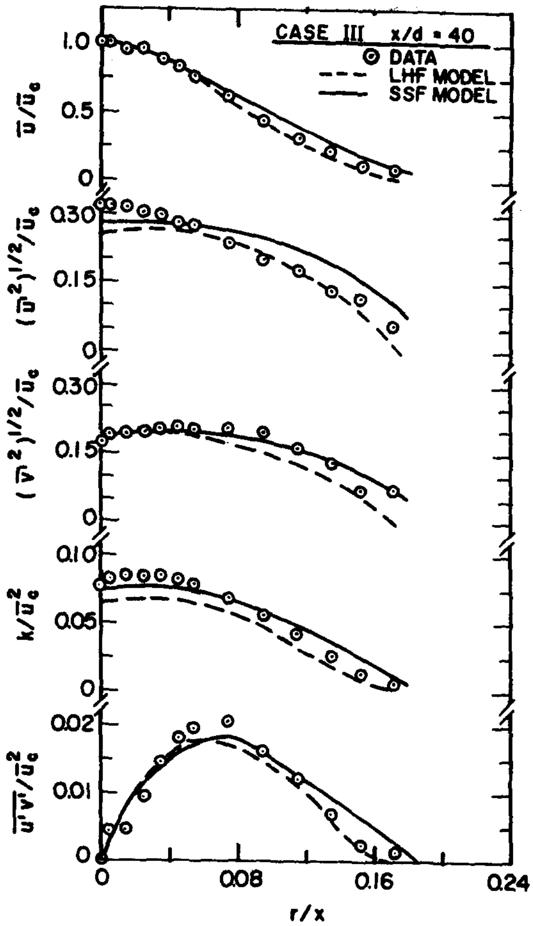

Figure 4. Mean and turbulent liquid-phase properties for the case III bubbly jet at $x/d = 40$.

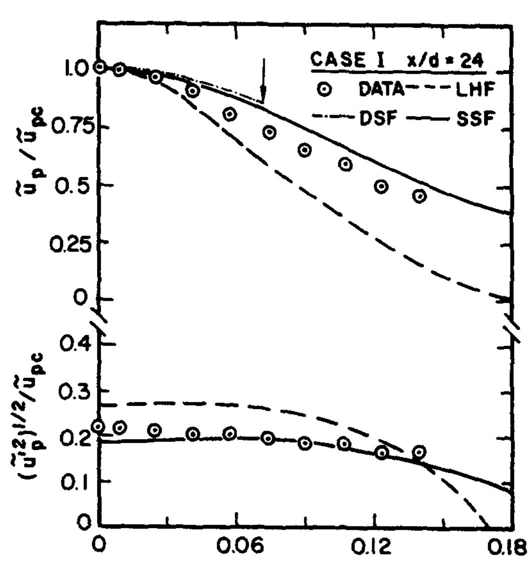

Figure 5. Mean and fluctuating bubble-phase velocities for the case I bubbly jet at $x/d = 24$.

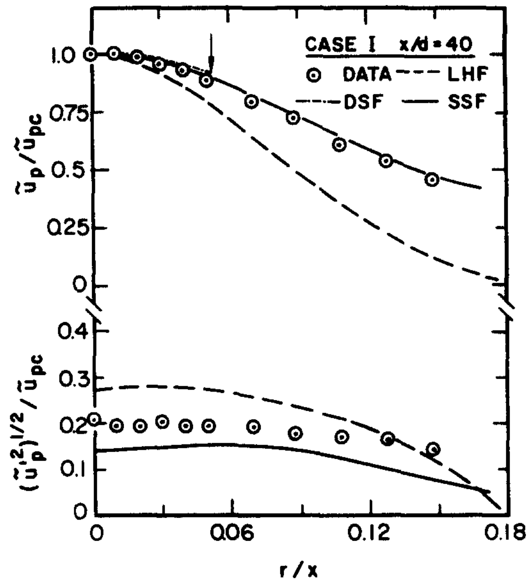

Figure 6. Mean and fluctuating bubble-phase velocities for the case I bubbly jet at $x/d = 40$.

processes in a laminar jet; therefore, bubbles only move in the radial direction as a result of drag forces from mean radial velocities of the continuous phase (aside from any initial radial bubble velocities which rapidly decay). These velocities are small in comparison to radial velocity fluctuations in turbulent jets; therefore, turbulent dispersion dominates the process. Furthermore, the laminar-like treatment results in disconcerting accumulations of bubbles where the mean radial velocity is zero, e.g., near the centerline (unstably) and near the point of inflection of the mean continuous-phase velocity profile (stably). Soo (1967) gives a number of examples of these dispersed-phase concentration effects in laminar flows. Present DSF predictions only exhibited these effects by the slow rate of spread of the dispersed phase from the axis, since the length of the region where measurements were made was relatively small. Certainly, this behavior represents a major deficiency of the DSF approach.

The results illustrated in figures 5–8 also show a major deficiency of the LHF approach.

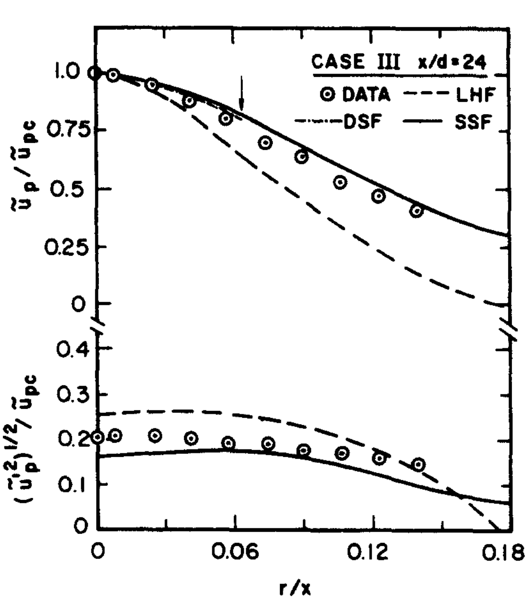

Figure 7. Mean and fluctuating bubble-phase velocities for the case III bubbly jet at $x/d = 24$.

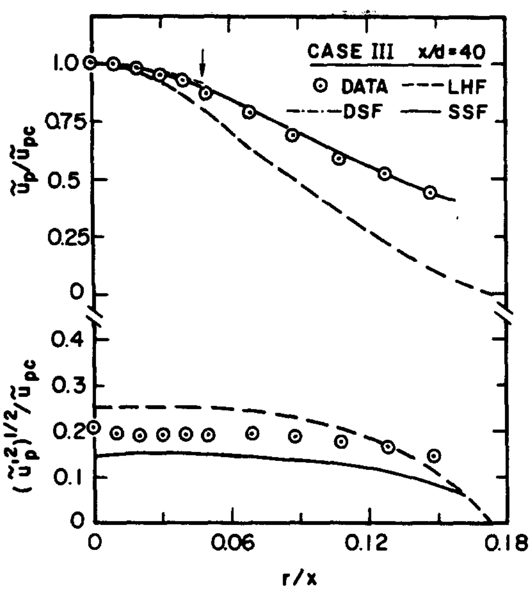

Figure 8. Mean and fluctuating bubble-phase velocities for the case III bubbly jet at $x/d = 40$.

The LHF analysis ignores relative velocity and yields best results in regions where relative velocities are small in comparison to mean continuous-phase velocities. Near the edge of the jet, however, liquid velocities are low since the ambient fluid is stagnant. Therefore, the LHF analysis significantly underestimates mean bubble velocities as the edge of the flow is approached. It should also be noted that earlier LHF predictions of bubble velocities along the flow axis were also not very accurate (Sun & Faeth 1985), since liquid velocities were relatively low for present test conditions.

In contrast to the other methods, the SSF analysis yields reasonably good predictions of mean bubble velocities, since effects of both turbulent dispersion and relative velocity are considered. This approach also yielded good mean bubble velocity predictions along the axis; therefore, absolute bubble velocities as well as the normalized values illustrated in figures 5–8 were satisfactory.

Measured streamwise bubble velocity fluctuations are overestimated by the LHF analysis and underestimated by the SSF analysis. Ignoring effects of relative velocities appears to be the main problem with the LHF analysis. This causes mean bubble velocities to be high in comparison to velocity fluctuations in the continuous phase, which are the source of velocity fluctuations of bubbles.

Three explanations can be advanced for the underestimation of bubble velocity fluctuations by the SSF analysis—aside from general uncertainties of turbulence models concerning predictions of turbulence properties. First of all, bubble diameters were not precisely constant which causes variation of terminal velocities, broadening velocity fluctuation levels from predictions based on constant bubble diameters. Approximate analysis indicates that this would explain about a third of the difference between SSF predictions and measurements seen in figures 5–8. Gradient broadening of the measurements is another potential source for increased measured bubble velocity fluctuations, however, calculations showed that this effect was small for present conditions. A defect of SSF analysis, advanced earlier by Shuen *et al.* (1983, 1983a, 1985) in connection with particle-laden jets, is also a factor. This involves the assumption of isotropic turbulence when randomly selecting eddy properties in the SSF simulations even though effects of anisotropy of the continuous phase are present, cf. figures 1–4.

Anisotropic SSF analysis is a feasible extension of present methods, e.g., the velocity PDFs for each component could be assigned different variances. However, such a tactic

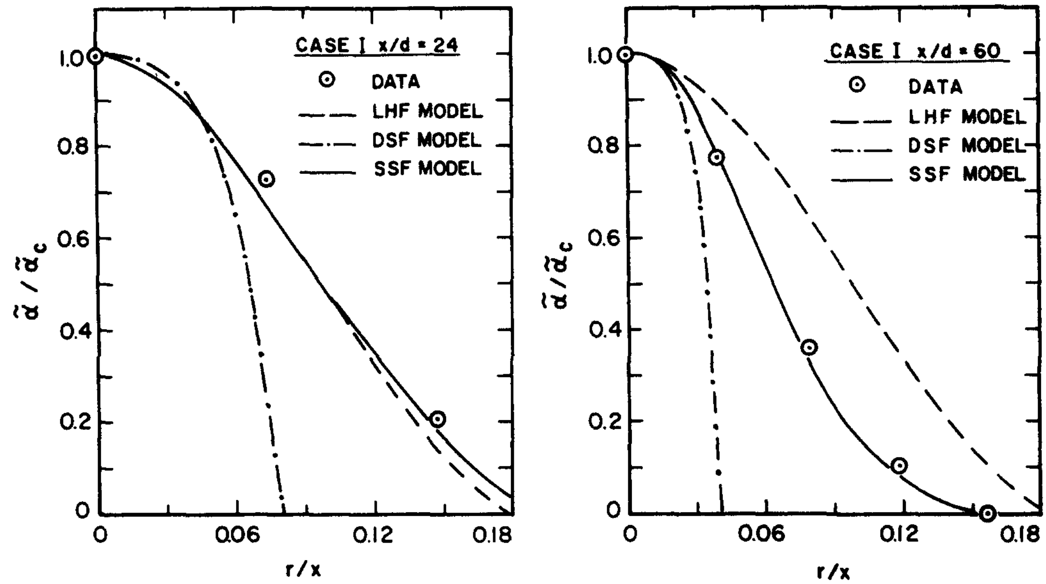

Figure 9. Mean bubble number intensity distributions for the case I bubbly jet.

would be *ad hoc*, and not representative of all levels of anisotropy along a radius, unless a multistress turbulence model was used. Development of a multistress model is beyond the scope of the present study, but appears to be a needed extension.

Distribution of bubbles. Mean bubble number intensity, $\tilde{\alpha}$, distributions for the case I and III bubbly jets at $x/d = 24$ and 60 are illustrated in figures 9 and 10. The measurements represent the number of bubbles per unit area along a path through the flow, parallel to the optical axis of observation, at various radial distances. Predictions of this quantity for all three methods of analysis are also illustrated on the figures.

The LHF predictions illustrated in figures 9 and 10 are reasonably good near the injector, where relative velocities are small in comparison to flow velocities. Far from the injector, however, the LHF analysis overestimates bubble dispersion, due to underestimation of streamwise bubble velocities and overestimation of bubble velocity fluctuations, by

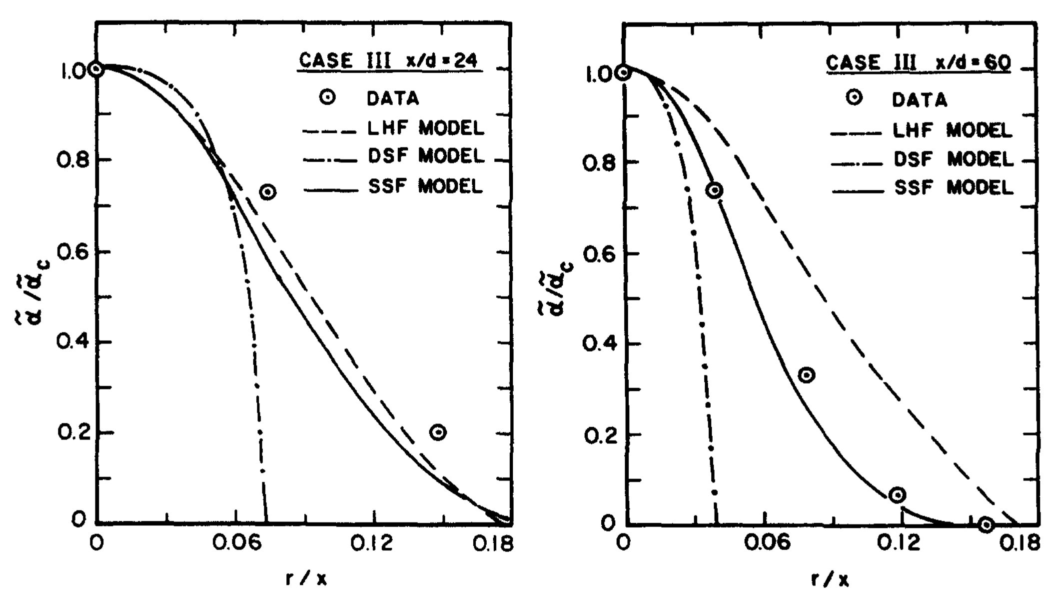

Figure 10. Mean bubble number intensity distributions for the case III bubbly jet.

neglecting relative velocity effects. On the other hand, the DSF approach underestimates the dispersion of bubbles everywhere, since bubble/turbulence interactions, which dominate the spread of the dispersed phase, are ignored.

In contrast to the other two methods, the SSF analysis provides reasonably good predictions of bubble number intensity distributions illustrated in figures 9 and 10. This is encouraging, since the distribution of bubbles is an important property of bubbly jets which strongly influences their structure. The present findings also illustrate the clear need for treating effects of turbulent dispersion of bubbles other than by some sort of similarity correlation often used in integral analysis of bubbly flows. Near the injector, bubbles tend to follow liquid fluctuations since maximum relative velocities are small in comparison to liquid velocities. Far from the injector, however, relative velocities are large in comparison to liquid velocities and effects of turbulent dispersion progressively decrease. The SSF analysis can simulate this transition in effects of turbulent dispersion while the LHF and DSF methods can only bound dispersion effects.

Shuen *et al.* (1984) observed somewhat different effects of turbulent dispersion in particle-laden jets than the present bubbly jets. For particle-laden jets, realtive velocities are large and turbulent dispersion effects are small near the injector since drop inertia limits response to fast rates of flow deceleration and small-length-scale turbulent fluctuations near the injector. Farther downstream, regimes are encountered where relative velocity effects are less important followed by a final relative-velocity-dominated flow as particles approach their terminal velocities in a relatively slow-moving continuous phase. Since bubble inertias are small, only the latter two regions are observed for bubbly jets. This accounts for the reasonable success of LHF analysis near the injector for bubbly jets, paralleled by similar success for DSF analysis of near-injector processes of particle-laden jets and sprays. The value of the SSF analysis is that it can bridge these regions with only a modest intrusion of new empiricism and with no change in empirical parameters for flows as disparate as bubbly and particle-laden jets.

2.3 *Turbulence modulation*

The maximum ratio of gas-to-liquid volume flow rates for present test conditions is on the order of 10^{-4} (at $x/d = 24$). For such conditions, it is reasonable to ignore direct contributions of interphase transport on the turbulence properties of the continuous phase. Certainly, predictions discussed thus far for the SSF analysis yielded encouraging agreement with measurements without considering the effect. Nevertheless, it is of interest to apply methods developed by Shuen *et al.* (1985) to treat turbulence modulation, using SSF analysis, in order to sutdy the effect more quantitatively.

Shuen *et al.* (1985) derived source terms in the governing model equations for k and ϵ, due to dispersed phase/turbulence interactions, as follows:

$$k\text{-equation: } \overline{uS_{pu}} - \bar{u}\,\bar{S}_{pu}, \qquad [2]$$

$$\epsilon\text{-equation: } -2\,C_{\epsilon 3}\,\mu_t\,\frac{\epsilon}{k}\,\frac{\partial \bar{S}_{pu}}{\partial r}, \qquad [3]$$

where u is the streamwise continuous-phase velocity, S_{pu} is the interphase momentum transport per unit volume, μ_t is the turbulent viscosity and $C_{\epsilon 3}$ is an empirical constant. The overbars indicate time-averages, which are appropriate since the continuous-phase density is constant and void fractions are small. The new term in the k-equation can be evaluated exactly using the SSF analysis. Typical of higher-order turbulence models, however, the new term in the ϵ-equation must be modeled, requiring the one new model constant, $C_{\epsilon 3}$. The value of $C_{\epsilon 3}$ is not known very well, although existing evidence suggests values in the range 0.1–1.0

(Shuen *et al.* 1985). Calculations during this investigation considered values of 0.2 and 0.8, as limits.

Percent changes in $\bar{u}_c$, $(k/\bar{u}^2)_c$, $\overline{u'v'}_{max}/\bar{u}_c^2$ and $\bar{u}_p$ between SSF analysis with and without the source terms of [2] and [3] are summarized in table 1 for $C_{\epsilon3} = 0.2$. Effects of turbulence modulation increase with increasing void volume, distance from the injector and values of $C_{\epsilon3}$. For mean quantities, $\bar{u}_c$ and $\bar{u}_{pc}$, the effect is less than 4%. The effect of turbulence modulation is greater for turbulence quantities, e.g., up to an 18% increase in $k_c/\bar{u}_c^2$ and a 11% increase for $(\overline{u'v'})_{max}/\bar{u}_c^2$. The best match of present measurements was achieved using $C_{\epsilon3} = 0.2$, which can rectify discrepancies between predicted and measured continuous-phase properties illustrated in figures 1–4. However, these changes are less than experimental uncertainties and this assessment of $C_{\epsilon3}$ is not very definitive.

For present conditions, predicted effects of turbulence modulation increase with increasing distance from the injector, even though void volumes are decreasing (quadratically with distance) at the same time. This occurs, since the present jets are dominated by relatively large bubble terminal velocities far from the injector. The resulting increases in turbulence levels cause the continuous-phase flow field to spread more rapidly, which decreases continuous-phase velocities and, to a lesser degree, mean bubble velocities.

2.4 *Sensitivity study*

The sensitivity of SSF predictions to uncertainties in initial conditions and model parameters was also studied. Four parameters were considered: k_0, ϵ_0, C_D and d_p. Sensitivity of k_0 and ϵ_0 was examined since initial-condition measurements of these quantities were made where experimental uncertainties were highest for turbulence quantities. C_D and d_p were considered since calibration of bubble drag can be influenced by surface active agents and bubble diameters were not truly monodisperse in the present flows.

Results of the sensitivity study are summarized in table 2. Quantities tabulated are the percent change in the computed output variable for a 100% increase of the input variable. Results are provided for the case I and III bubbly jets at $x/d = 24$, which is the location where sensitivities were greatest. The most sensitive output variables are shown, e.g., $\bar{u}_c$, $(k/\bar{u}^2)_c$, $\bar{u}_{pc}$ and $(\bar{u}_p'/\bar{u}_p)_c$. The properties of the continuous phase were essentially independent of uncertainties of the dispersed phase, since present flows were dilute. Even large (100%) changes in d_p and C_D had relatively small influence on predictions of mean and fluctuating bubble velocities as well, e.g., less than 20%. Effects of uncertainties in k_0 and ϵ_0 are greater, since present measurements are in the transitional flow development region of bubbly jets. In this case, uncertainties in k_0 are translated directly into uncertainties in k at $x/d = 24$, although this influence declines at larger distances from the injector. However, effects of k_0 and ϵ_0 are smaller concerning mean liquid velocities and bubble properties—not exceeding 35%. In general, we conclude that uncertainties in initial conditions, C_D and d_p

Table 1. Turbulence modulation study of SSF analysis†

x/d	$C_{\epsilon3}$	$\bar{u}_c$	$k_c/\bar{u}_c^2$	$(\overline{u'v'})_{max}/\bar{u}_c^2$	$\bar{u}_{pc}$
Case I:					
24	0.2	−0.0	0.6	0.3	−1.4
	0.8	−0.6	2.3	1.3	−6.4
40	0.2	−0.4	1.3	0.8	1.1
	0.8	−1.1	5.1	2.9	−0.2
Case III:					
24	0.2	−0.2	1.5	1.0	−2.3
	0.8	−1.3	7.4	5.5	−2.8
40	0.2	−0.6	4.6	2.7	−3.8
	0.8	−3.5	18.1	10.9	−0.5

†*Percent increase of parameter upon including turbulence modulation terms.*

Table 2. Sensitivity study of SSF analysis†

Input Parameter	Output Parameter			
	$\bar{u}_c$	$(k/\bar{u}^2)_c$	$\bar{u}_{pc}$	$(\bar{u}'_p/\bar{u}_p)_c$
Case I:				
k_o	−35	119	−25	29
ϵ_o	32	−44	21	−18
C_D	−0	−0	−8	10
d_p	−0	−0	16	−20
Case III:				
k_o	−35	109	−26	34
ϵ_o	32	−41	23	−17
C_D	−0	−0	−7	11
d_p	−0	−0	14	−18

†Percent increase in output parameter at $x/d = 24$ for a 100% increase in input parameter.

should not influence computed output beyond the estimated uncertainty of the structure measurements—roughly 5% for mean quantities and turbulent fluctuations, 10% for k and 20% for the Reynolds stress.

2.5 *Length scales*

Although predictions using the SSF approach were encouraging, one aspect of the evaluation raises some concerns. The original development of the method by Gosman & Ioannides (1981) and Shuen *et al.* (1983, 1983a, 1985) considered particle-laden flows and sprays where dimensions of the dispersed phase were small in comparison to the smallest turbulence scales (Faeth 1983). This condition, however, was not satisfied for the present bubbly jets even though bubble diameters were only 1 mm. For example, L_e/d_p, where L_e is the characteristic eddy size used in the SSF simulation, ranged from 0.5–5 for present conditions, with smallest values near the injector. Since bubble sizes are significant in comparison to turbulent scales, this yields a much different picture of the interaction between bubbles and turbulent eddies than the point-particle ideas considered for particle-laden flows. The success of the the SSF method in spite of this may be due to the fact that effects of relative velocity were small near the injector where L_e/d_p is smallest. Another factor is that L_e serves primarily as a measure of perhaps larger turbulent scales which are actually responsible for turbulent dispersion. Extension of the SSF method to other flow geometries should be approached with caution as a result, since the method has only been evaluated for jet-like flows which tend to have similar distributions of scales.

Another aspect of the relatively large bubble sizes in comparison to turbulence scales is that use of drag coefficients from low turbulence intensity flows may no longer be appropriate (Faeth 1983). A mitigating feature in the present case, however, is the relative insensitivity of the predictions to uncertainties in bubble drag (discussed in section 2.4).

3. CONCLUSIONS

The conclusions of the study are as follows:

(1) Effects of relative velocity were small near the injector (except near the edge of the flow) but begin to dominate the flow far from the injector ($x/d > 24$), while effects of turbulent dispersion were important everywhere.
(2) The LHF analysis, which ignores the relative velocity but considers turbulent dispersion, and the DSF analysis, which considers relative velocity but ignores turbulent dispersion yielded poor results for present conditions and appear to have limited value for analyzing bubbly jets.
(3) In contrast, the SSF approach yielded encouraging predictions over the present data

base, with no change in the prescription of turbulence model constants or eddy properties from its original use in particle-laden flows.

(4) Effects of turbulence modulation were not very significant for present flows since void volume fractions were less than 10%.

(5) Sensitivity analysis indicated that uncertainties in initial conditions, bubble drag coefficients and variations in bubble sizes should not influence SSF predictions beyond the estimated uncertainty of the measurements.

(6) Turbulence scales were not small in comparison to bubble diameters for present test conditions, especially near the injector exit; therefore, present conditions are far different from the point particle/large eddy interactions envisioned when the SSF analysis was originally developed for particle-laden jets. The encouraging performance of the SSF analysis in spite of this probably resulted from effects of low relative velocity near the injector, where this ratio was lowest.

(7) Effects of anisotropy of turbulence properties on bubble velocity fluctuations were observed, which were not treated in analyses considered here. Treating this effect will require a multistress turbulence model or a full simulation of the turbulent flow field.

Acknowledgments—This research was supported by the Office of Naval Research, Contract No. N00014-80-C-0517 under the technical management of R. D. Ryan. The authors acknowledge the valuable help of L-D. Chen and J-S. Shuen during development of the analysis.

REFERENCES

AL TAWEEL, A. M. & LANDAU, J. 1977 Turbulence modulation in two-phase jets. *Int. J. Multiphase Flow* **3**, 341–351.

FAETH, G. M. 1983 The evaporation and combustion of sprays. *Prog. Energy Combust. Sci.* **9**, 1–76.

GOSMAN, A. D. & IOANNIDES, E. 1981 Aspects of computer simulation of liquid-fueled combustors. AIAA Paper No. 81-0323.

JENG, S-M. & FAETH, G. M. 1984 Species concentrations and turbulence properties in buoyant methane diffusion flames. *J. Heat Transfer* **106**, 721–727.

SHUEN, J-S., CHEN, L-D. & FAETH, G. M. 1983 Evaluation of a stochastic model of particle dispersion in a turbulent round jet. *A.I.Ch.E.J.* **29**, 167–170.

SHUEN, J-S., CHEN, L-D. & FAETH, G. M. 1983a Predictions of the structure of turbulent, particle-laden, round jets. *A.I.A.A.J.* **21**, 1480–1483.

SHUEN, J-S., SOLOMON, A. S. P., ZHANG, Q-F. & FAETH, G. M. 1985 Structure of particle-laden jets: measurements and predictions. *A.I.A.A.J.* **23**, 396–404.

SOLOMON, A. S. P., SHUEN, J-S., ZHANG, Q-F. & FAETH, G. M. 1984 Structure of nonevaporating sprays: measurements and predictions. AIAA Paper No. 84-0125.

SOO, S. L. 1967 *Fluid Dynamics of Multiphase Systems*. Blaisdel, Waltham, MA.

SUN, T-Y. 1985 A theoretical and experimental study of noncondensible turbulent bubbly jets. Ph.D. Dissertation, The Pennsylvania State University, University Park, PA.

SUN, T-Y. & FAETH, G. M. 1985 Structure of turbulent bubbly jets—I. methods and centerline properties. *Int. J. Multiphase Flow* **12**, 99–114.

WYGNANSKI, I. & FIEDLER, H. E. 1969 Some measurements in the self-preserving jet. *J. Fluid Mech.* **38**, 577–612.